SELECTIVE 'COMPLEX' REFLECTIONLESS POTENTIALS

By

Andrew Hasenfeld

IMA Preprint Series # 439

August 1988

SELECTIVE 'COMPLEX' REFLECTIONLESS POTENTIALS

ANDREW HASENFELD†

Abstract. Previous results obtained in attempts to invert the Bloch transform for the reduced case of amplitude modulation are extended to the general case of simultaneous amplitude and phase modulation. Numerical results are presented which illuminate this general case, and these results are interpreted in terms of one-dimensional non-relativistic quantum mechanical scattering. We find that the full (complex) case of simultaneous amplitude and phase modulation is more robust than the reduced (real) case of amplitude modulation.

1. Preamble. This lecture should be viewed as a companion to the one entitled "Soliton Mathematics in Signal Processing" by F. Alberto Grünbaum [1]. Indeed, the numerical results presented here, along with the experimental verification contained in [5], stimulated much of the new perspective provided by [1]. Before elaborating on the title of this paper, a few remarks should be addressed to the current situation.

A nice feature of the inverse scattering reformulation of the NMR "selective excitation" issue is in its physical motivation. The concerns fundamental to this NMR problem are nonlinear, and so borrowing techniques from the nonlinear wave community should be seen as natural, and moreover physically intuitive. In particular, the general prescription of viewing the desired response (namely the amplitude and phase modulations of the imposed radiofrequency field that achieve a given excitation profile) as comprising scattering data, and the unknown modulations as sitting in the potential that produces that scattering data, is an appealing metaphor for getting a handle on the relevant questions and their solutions.

We close this brief sermon with a few remarks concerning the many unexplained mysteries run into along the tortuous path to this point (perhaps the words "conspiracy of miracles" describe it best), and some deeply felt thanks for the pioneering work of G.L. Lamb, Jr. (referenced in [1]). One would like to have a clear physical picture of the many exotic phenomena exhibited by simple spin systems, not only encompassing the miraculous response of self-induced transparency [6], but also the rectangular inversions described here. The inverse scattering perspective unifies the explanations for these things under one umbrella, so that the generalization from pure amplitude modulation to simultaneous amplitude and phase modulation comes with a nice physical meaning (corresponding to the transition from a real-valued to a complex-valued potential in the associated scattering picture). As we will show in section 7, this approach is equivalent to the general framework constructed by physicists to describe statistical ensembles of spins [10], and so in principle should describe all of the relevant phenomena. Finally, it should be stated that there exist other approaches to the solution of this problem, most notably the one arising from ideas in optimal control [7].

†Department of Chemistry, Princeton University, Princeton, NJ 08544. This work was supported by the National Institutes of Heath under grant GM35253 BBCB, and by the National Science Foundation under grant CHE-8502199.
Present address: Center for Pure and Applied Mathematics, University of California, Berkeley, CA 94720.

2. Formal introduction. We have written at length about attempts to invert a complicated nonlinear map called the Bloch transform ([2-4] and references therein) in the reduced case of amplitude modulation. This transformation

$$\mathcal{B}: \gamma \mathrm{H}_1(t) = \omega_1(t) e^{i\varphi(t)} \rightarrow \mathrm{M}(\Delta\omega, T) \tag{2.1}$$

represents integration of the Bloch equations, where the pulse of radiation lasts in time t from 0 to T, and $\Delta\omega$ is a parameter called the resonance offset (linearly proportional to distance). The underlying physical motivation in all of this work has been to comprehend the quantum mechanical interaction of electromagnetic radiation with spin, and the use of the language of inverse scattering has provided a backdrop upon which to realize an appropriate description. Most recently, we have had success extending the formalism to the general case of simultaneous amplitude and phase modulation [5], and it is now clear that viewing $\mathcal{B}^{-1}$ as an analogue of the inverse scattering transform is both fruitful and remarkably accurate. One sees that the general case follows as a simple extension of the scattering formalism to scattering in the presence of a complex potential.

We will begin with an analytical treatment of the simple quantum mechanical equations of motion for an isolated two-level system in an external field. We then move to a consideration of numerical findings (in an attempt to identify the subset of reflectionless potentials that produce 'rectangular' inversion profiles), using some remarkably simple arguments from one-dimensional non-relativistic quantum mechanical Schrödinger scattering for an interpretation of the dynamics of uncoupled two-level systems. Finally, we connect the two component formulation of Zakharov and Shabat to the physicists' language of the density matrix. Some mysteries still remain, but we are now confident that our elementary scattering viewpoint can ultimately handle them.

3. Bloch → Riccati → Schrödinger. We now describe a certain mathematical pathway which, in the reduced case of amplitude modulation, led to a successful description (see [2-4]). In trying to extend this method to the general situation embodied in (3.1), however, one runs into problems that cannot be ignored. Nevertheless, it is instructive to see how it all breaks down.

We begin with the Bloch equations for amplitude and phase modulation

$$\frac{d}{dt}\begin{pmatrix} M_x \\ M_y \\ M_z \end{pmatrix} = \begin{pmatrix} 0 & \Delta\omega & -\omega_1(t)\sin\varphi(t) \\ -\Delta\omega & 0 & \omega_1(t)\cos\varphi(t) \\ \omega_1(t)\sin\varphi(t) & -\omega_1(t)\cos\varphi(t) & 0 \end{pmatrix}\begin{pmatrix} M_x \\ M_y \\ M_z \end{pmatrix} \tag{3.1}$$

with the initial condition $\mathbf{M}(\Delta\omega,0)=(0,0,-1)^T$, and where relaxation terms are neglected. By stereographically projecting $\mathbf{M}$ onto the y-z plane

$$\eta(\Delta\omega, t) = \frac{M_z + iM_y}{M_x - 1}, \tag{3.2}$$

we find that η satisfies a Riccati equation

$$\begin{aligned} \dot{\eta} &= \left(\frac{\omega_1 \sin\varphi + i\Delta\omega}{2}\right)\eta^2 + (i\omega_1\cos\varphi)\eta + \left(\frac{\omega_1\sin\varphi - i\Delta\omega}{2}\right) \\ &= a\eta^2 + b\eta + c. \end{aligned} \tag{3.3}$$

(Here is one of the mysteries: why does stereographic projection yield a Riccati equation?) The general approach is then to construct a

$$g \equiv e^{-\int_{-\infty}^{t}(a\eta+\frac{\dot{a}}{2a}+\frac{b}{2})} \tag{3.4}$$

to linearize (3.3) into the form

$$\begin{aligned} -\ddot{g} &= -\frac{1}{4}[3(\frac{\dot{a}}{a})^2 - \frac{2\ddot{a}}{a} + \frac{2\dot{a}b}{a} + b^2 - 4ac - 2\dot{b}]g \\ &= [E - V_1 - V_2]g \end{aligned} \tag{3.5}$$

with

$$\begin{gathered} V_1 = \tfrac{1}{4}[3(\tfrac{\dot{a}}{a})^2 - \tfrac{2\ddot{a}}{a} + \tfrac{2\dot{a}b}{a}] \\ V_2 - E = \tfrac{1}{4}[b^2 - 4ac - 2\dot{b}] \\ a = \tfrac{\omega_1 \sin\varphi + i\Delta\omega}{2} \\ b = i\omega_1 \cos\varphi \\ c = a^* = \tfrac{\omega_1 \sin\varphi - i\Delta\omega}{2} \end{gathered} \tag{3.6}$$

In this form, by replacing t by a spatial parameter $\overline{x}$, we arrive at the "time-independent" Schrödinger equation

$$-\frac{d^2g}{d\overline{x}^2} + (V - E)g = 0, \tag{3.7}$$

where one identifies the energy E and the potential V as

$$\begin{gathered} V - E = V_1 + V_2 - E = \tfrac{1}{4}[3(\tfrac{\dot{a}}{a})^2 - \tfrac{2\ddot{a}}{a} + \tfrac{2\dot{a}b}{a} + b^2 - 4ac - 2\dot{b}] \\ E \equiv \lambda^2 = (\tfrac{\Delta\omega}{2})^2 \end{gathered} \tag{3.8}$$

At this point, we run into difficulties. When $\varphi \equiv 0$ (amplitude modulation), we see from (3.6) that V_1 vanishes identically, and that V_2-E becomes

$$V_2 - E = -\frac{1}{4}[\omega_1^2 + 2i\dot{\omega}_1 + \Delta\omega^2]. \tag{3.9}$$

From the argument in [3], the term $-\frac{i\dot{\omega}_1}{2}$ is neglected, and so the ansatz

$$\omega_1 \sim \sqrt{-V(\overline{x})} \tag{3.10}$$

results. In the general case (3.1), however, V_1 no longer vanishes, and (as noted in [1]) our simple inverse scattering picture based on the Schrödinger equation begins to unravel.

However, proceeding ahead blindly, we evaluate

$$V_2 - E = -(\frac{\omega_1}{2})^2 - i\frac{\dot{\omega}_1 \cos\varphi}{2} + i\frac{\omega_1\dot{\varphi}\sin\varphi}{2} - (\frac{\Delta\omega}{2})^2. \tag{3.11}$$

Recall we wish to reconstruct ω_1 and φ from the real and imaginary parts of V. But if

$$\dot{\omega_1} \sim \omega_1 \dot{\varphi}, \tag{3.12}$$

from (3.6) and (3.8) we have

$$Re(V_2) \sim -(\frac{\omega_1}{2})^2 \, , \, Im(V_2) \sim -\frac{\dot{\omega_1}}{2}(\cos\varphi - \sin\varphi). \tag{3.13}$$

Now (3.12) is easy to integrate

$$\varphi = \mu \, ln(\omega_1), \tag{3.14}$$

for constant μ, which yields the ansatz

$$\gamma H_1(t) = \omega_1 e^{i\mu \, ln(\omega_1)} = \omega_1^{(1+\mu i)} \sim (\sqrt{-V})^{(1+\mu i)}. \tag{3.15}$$

Call it divine inspiration, but the rest of this paper will present some very surprising numerical results using this ansatz (3.15), and we will also interpret the results in the language of one-dimensional Schrödinger scattering. The mystery here concerns the neglect of the terms in V_1, together with the simple explanation of these results in terms of a Schrödinger picture. Yet as we shall see in section 7, a two component formulation is able to account for this omission nicely.

4. Asymptotics. By examining the large positive and negative $\overline{x}$ (equivalently t) behavior of g in (3.4), we see that

$$g \sim \begin{cases} e^{-i\lambda\overline{x}}, & \text{as } \overline{x} \to -\infty \\ pe^{-i\lambda\overline{x}} + se^{i\lambda\overline{x}}, & \text{as } \overline{x} \to \infty \end{cases} \tag{4.1}$$

since V$\to$0 as $\overline{x} \to \pm\infty$, and because of the initial condition M($\Delta\omega$,0)=(0,0,-1)^T. By also imposing boundary conditions on the bound states (E=-λ_i^2, λ_i >0, i=1,...,N)

$$g \sim \begin{cases} e^{\lambda\overline{x}}, & \text{as } \overline{x} \to -\infty \\ s_i(\lambda_i)e^{-\lambda\overline{x}}, & \text{as } \overline{x} \to \infty \end{cases} \tag{4.2}$$

for s_i the i^{th} normalization constant, we have translated the Bloch evolution in t into a Schrödinger scattering problem in $\overline{x}$ (note that the interval [0,T] is replaced by $[-\infty, \infty]$) in which a plane wave is incident with amplitude p from the right, and gets transmitted with unit amplitude and reflected with amplitude s.

We can say more, by examining the large t behavior of $\frac{\dot{g}}{g}$. From the definition of g in (3.4), we see that

$$\frac{\dot{g}}{g} \sim -i\lambda\eta = -i\lambda\frac{M_z + iM_y}{M_x - 1} \tag{4.3}$$

and on the other hand, from (4.1)

$$\frac{\dot{g}}{g} \sim -i\lambda \frac{pe^{-i\lambda t} - se^{i\lambda t}}{pe^{-i\lambda t} + se^{i\lambda t}}. \tag{4.4}$$

Moreover, at large t, from (3.1) it is easy to see that

$$\begin{aligned} M_x(2\lambda,t) &= \tfrac{m_x}{2}(e^{2i\lambda t} + e^{-2i\lambda t}) + \tfrac{m_y}{2i}(e^{2i\lambda t} - e^{-2i\lambda t}) \\ M_y(2\lambda,t) &= \tfrac{m_y}{2}(e^{2i\lambda t} + e^{-2i\lambda t}) - \tfrac{m_x}{2i}(e^{2i\lambda t} - e^{-2i\lambda t}). \\ M_z(2\lambda,t) &= m_z \end{aligned} \tag{4.5}$$

Substituting (4.5) into (4.3) and cross-multiplying, when the dust settles one finds the eight conditions

$$\begin{array}{ll} -\frac{m_x s}{2} = -\frac{m_x s}{2} & \frac{m_x p}{2} = \frac{m_x p}{2} \\ \frac{m_y s}{2} = \frac{m_y s}{2} & \frac{m_y p}{2} = \frac{m_y p}{2} \\ \frac{m_y s}{2} = -\frac{m_y s}{2} & \frac{m_y p}{2} = -\frac{m_y p}{2} \\ m_z s - \frac{m_x p}{2} = s + \frac{m_x p}{2} & m_z p + \frac{m_x s}{2} = -p - \frac{m_x s}{2} \end{array}, \tag{4.6}$$

with only two possible solutions:
(i) p=0 and $M_z = m_z$=1, and
(ii) s=0 and $M_z = m_z$=-1.
We discuss these two cases in turn.

Examining (4.1) when p vanishes, the potential V becomes 'super-radiant', in the sense that no wave impinges on V, but there exist outgoing waves in both directions. While this is unusual physical behavior, it is allowed when V is complex, and so the inverted state M_z=1 corresponds to a situation in which waves emanate from V in both directions, even though no wave is incident.

Conversely, when s vanishes, from (4.1) we see that the potential V is "reflectionless", since this time the plane wave propagates unimpeded through V, and no part of the wave is reflected. This case is identical to the previous results for amplitude modulation [4], that V is a reflectionless potential [8].

We close this section with a brief summary of how one computes such reflectionless V. The determinant of the matrix

$$A_{ij} = \delta_{ij} + \frac{s_i}{\lambda_i + \lambda_j} e^{-(\lambda_i + \lambda_j)\overline{x}} \tag{4.7}$$

is differentiated to obtain

$$V(\overline{x}) = -2\frac{d^2}{d\overline{x}^2} \ln\, det(A(\overline{x})). \tag{4.8}$$

5. Numerics. We show numerical simulations [9] of the Bloch equations (3.1) using the ansatz (3.15) with reflectionless V. While the analytic approach is exact in the limit as t ($=\overline{x}$) $\to \pm\infty$, in the finite digital simulations, the behavior is not perfect (i.e., there is a transition region from M_z=-1 to M_z=1). Nevertheless, as shown in figures 1 and 2, the behavior is very close to the limiting theoretical results.

In figures 3 and 4, we exhibit results for reflectionless potentials that do not achieve rectangular inversions. We find increased robustness in the parameter space ($\{\lambda_i, s_i\}$, i=1,...,N) compared to the real-valued case of amplitude modulation, so that now the result (equation (20) of [3])

$$| \lambda_{i+1} - \lambda_i | > O(1) \tag{5.1}$$

becomes

$$| \lambda_{i+1} - \lambda_i | > O(10^{-1}). \tag{5.2}$$

The general question raised in [3] remains: namely, what values of the 2N parameters $\{\lambda_i, s_i\}$ that determine a particular reflectionless V produce "good" NMR pulses? (The phase ϕ_i determines the position of the (i-1)th soliton).

One comment about our graphical display: in previous papers, we have usually shown 50 experiments in a single figure. However, in [3] we mention that this technique is misleading (it led to a misplaced correspondence with the Korteweg-de Vries equation), and so we now display a single reflectionless potential in each figure, to stress that the important object here is a set of 2N numbers, and not an isospectral flow of some nonlinear PDE.

6. Quantum mechanics. We will now give some arguments from non-relativistic quantum mechanics [11] to provide explanations of the observed numerical findings. The first is heuristic, to give a qualitative indication that we are on the right track. The other arguments are based on solid principles of non-relativistic quantum theory, and offer a perspective that we hope can explain all of the simple spin physics. There are also recent indications that some well-known approximation techniques, such as the Born approximation and the WKB method, can provide additional insight, but those approaches would take us too far afield here, and so will be discussed elsewhere.

One can understand the response purely in terms of scattering, with no need to appeal to the concept of adiabatic rapid passage [10]. Loosely speaking, think of the potential well V instead as a potential barrier of height $\sim \omega_1^2$, and the incident wave as having energy $\sim \Delta\omega^2$. The wave will be exponentially damped if the energy in the wave is too small to get over the barrier (corresponding to M_z=1). Likewise, when the energy of the wave surpasses the height of the barrier, there is no reflection, and the wave propagates unimpeded (corresponding to M_z=-1). The transition occurs when the energy in the wave is close to the height of the barrier.

There is a second interpretation that reinforces our belief in the relevance of quantum scattering theory. One of the first computations done in learning about quantum theory is the derivation of the continuity equation for the probability amplitude $|\psi^*\psi|$ from the Schrödinger equation

$$i\hbar\frac{\partial\psi}{\partial t} = [-\frac{\hbar^2}{2m}\frac{\partial^2}{\partial x^2} + V(x)]\psi. \tag{6.1}$$

The usual result is

$$\frac{\partial \rho}{\partial t} + \frac{\partial}{\partial x} \mathrm{S} = 0, \tag{6.2}$$

where

$$\rho = \int \psi^* \psi \, dx \, , \, \mathrm{S} = \frac{\hbar}{2im} \int (\psi^* \frac{\partial \psi}{\partial x} - (\frac{\partial \psi^*}{\partial x}) \psi) \, dx, \tag{6.3}$$

which is obtained when the potential V is real-valued. In the more general case of complex V, the zero on the r.h.s. of (6.2) is replaced by the source term $\frac{2}{\hbar}\mathrm{Im(V)}$. Now, from (3.12-14), it is easy to see that our Im(V) scales linearly with μ, so that as μ increases, so does the production of probability in the state M_z=1. Therefore, the size of the inverted region increases (linearly with μ!), as seen in figure 1.

The final argument says that our analogy to quantum mechanics is really one-dimensional. It is a consequence of the general properties of the motion in one dimension that the spectrum of discrete bound states, or negative energy levels, is nondegenerate. (An equivalent statement is that the Wronskian of two different eigenfunctions corresponding to the same negative value of energy vanishes identically in one dimension). But this is *exactly* the phenomenon observed in figure 3, and formalized in (5.2).

Another mystery occurs at this point, as illustrated in figure 5. In the amplitude modulation case, one has an additional constraint (N denotes the number of bound states)

$$\int_{-\infty}^{\infty} \omega_1(t) \, dt = 2\pi N. \tag{6.4}$$

Therefore, in this reduced (real-valued) case, there is extreme "ω_1 sensitivity", namely that (6.4) must hold. In the general case (3.1), the constraint (6.4) disappears, and in its place one finds the opposite behavior, that the profile is insensitive to the strength of the irradiating radiofrequency field (equivalently, extreme "ω_1 insensitivity").

7. Density matrix. The two component formalism described in [1] is identical to that of a statistical operator ρ (called the density matrix [10]). Modulo factors of $\pm$i, and setting $\hbar$ and the gyromagnetic ratio γ everywhere to 1, this equivalence is given by

$$\rho \simeq P \equiv \sigma_1 M_x + \sigma_2 M_y + \sigma_3 M_z = \sigma \cdot \mathbf{M}. \tag{7.1}$$

Moreover, the time evolution for P (equation (9) in section 3 of [1]) is the same as the variation of ρ in time

$$\dot{\rho} = -[\mathcal{H}, \rho]. \tag{7.2}$$

We therefore see that the Hamiltonian $\mathcal{H}$ is identified with

$$\mathcal{H} \simeq -U'U^{-1} = -\sigma \cdot \mathbf{H}, \tag{7.3}$$

where **H** is the imposed magnetic field

$$\mathbf{H} = \begin{pmatrix} \omega_1(t)\cos\varphi(t) \\ \omega_1(t)\sin\varphi(t) \\ \Delta\omega \end{pmatrix}. \tag{7.4}$$

Thus the evolution of Zahkarov-Shabat type is the same as the density matrix motion (very similar to Heisenberg's equations of motion) for a statistical ensemble of free two-level spins.

If we try to write this evolution

$$\frac{d}{dt}\begin{pmatrix} v_1 \\ v_2 \end{pmatrix} = \begin{pmatrix} -i\zeta & q(t) \\ -q^*(t) & i\zeta \end{pmatrix}\begin{pmatrix} v_1 \\ v_2 \end{pmatrix} \tag{7.5}$$

in second order form, we have

$$-\ddot{v_1} + \frac{\dot{q}}{q}\dot{v_1} + (i\zeta\frac{\dot{q}}{q} - \zeta^2 + |q|^2)v_1 = 0. \tag{7.6}$$

Now, when N=1, our potential q is

$$q(t) = \frac{iA}{2}(sech\ \beta t)^{1+\mu i}, \tag{7.7}$$

so that

$$\frac{\dot{q}}{q} = -\beta(1+\mu i)\tanh\ \beta t. \tag{7.8}$$

Using a Liouville substitution

$$v_1 = ue^{-\frac{\beta}{2}(1+\mu i)\int^t \tanh\ \beta s\, ds}, \tag{7.9}$$

we finally obtain a Schrödinger equation

$$-\ddot{u}+[\frac{\beta^2}{4}(1+\mu i)^2\tanh^2\beta t - i\beta\zeta(1+\mu i)\tanh\ \beta t - \frac{A^2+2\beta^2(1+\mu i)}{4\cosh^2\beta t} - \zeta^2]u = 0 \tag{7.10}$$

with a potential hole of "modified" Pöschl-Teller type [12].

Finally, we consider the general problem (3.1) in a two component formalism, so that (7.5) becomes

$$\frac{d}{dt}\begin{pmatrix} v_1 \\ v_2 \end{pmatrix} = -\frac{i}{2}\begin{pmatrix} \Delta\omega & \omega_1 e^{i\varphi} \\ \omega_1 e^{-i\varphi} & -\Delta\omega \end{pmatrix}\begin{pmatrix} v_1 \\ v_2 \end{pmatrix} \tag{7.11}$$

with the potential q and energy ζ^2 given as

$$q(t) = -\frac{i\omega_1(t)}{2}e^{i\varphi(t)}\ ,\ \zeta = \lambda = \frac{\Delta\omega}{2}. \tag{7.12}$$

Defining $g=\frac{v_1+v_2}{2}$ in (3.5), we recover (3.11) exactly in the form

$$\ddot{g} = \frac{\ddot{v_1}+\ddot{v_2}}{2} = [-(\frac{\omega_1}{2})^2 - i\frac{\dot{\omega_1}\cos\varphi}{2} + i\frac{\omega_1\dot{\varphi}\sin\varphi}{2} - (\frac{\Delta\omega}{2})^2]g. \tag{7.13}$$

In addition, for the reduced case of pure amplitude modulation (i.e., $\varphi(t) \equiv 0$), this expression reduces to the Schrödinger form given in (3.9), namely

$$\ddot{g} = -\frac{1}{4}[\omega_1^2 + 2i\dot{\omega_1} + \Delta\omega^2]g. \tag{7.14}$$

8. Closing remarks. We have seen that non-relativistic scattering theory and uncoupled two-level system dynamics are intimately related. Indeed, we can see, by identifying the Zakharov-Shabat and density matrix formulations, that they are complementary views of a single phenomenon. Nevertheless, there are still some unresolved mysteries, and the complete picture remains unfinished.

The special initial and final states of the evolving magnetization we have considered has led to a large family of useful NMR pulses, namely those arising from the celebrated reflectionless potentials [8]. However, one would like to treat more general initial and final data for the magnetization M. While the Schrödinger formulation does appear tied to this reflectionless case, as we have seen in the previous section, a two component formulation of the inverse scattering problem arises as an equivalent representation to the density matrix. So one can look at two component versions of the inverse problem as a hopeful way to generalize this NMR reformulation to arbitrary configurations.

I gratefully acknowledge enlightening conversations with F.A. Grünbaum and W.S. Warren, and thank the Princeton Local Allocation Committee for five hours of supercomputer time at the John von Neumann Center, some of which was used in the development of the numerical evidence. Finally, I thank the officers and staff at the IMA for providing an extremely pleasant atmosphere in Vincent Hall.

REFERENCES

[1] F.A. Grünbaum, *Soliton Mathematics in Signal Processing (this volume).*

[2] F.A. Grünbaum and A. Hasenfeld, *An exploration of the invertibility of the Bloch transform*, Inverse Problems, 2 (1986), pp. 75–81.

[3] ———————, *An exploration of the invertibility of the Bloch transform: II*, Inverse Problems, 4 (1988), pp. 485-493.

[4] A. Hasenfeld, *A connection between the Bloch equations and the Korteweg-de Vries equation*, J. Magn. Reson., 72 (1987), pp. 509–521.

[5] A. Hasenfeld, S.L. Hammes, and W.S. Warren, *Understanding phase modulation in two-level systems through inverse scattering*, Phys. Rev. A (to appear).

[6] S.L. McCall and E.L. Hahn, *Self-induced transparency*, Phys. Rev., 183 (1969), pp. 457–485.

[7] J.B. Murdoch, A.H. Lent, and M.R. Kritzer, *Computer-optimized narrowband pulses for multislice imaging*, J. Magn. Reson., 74 (1987), pp. 226–263.

[8] V. Bargmann, *On the connection between phase shifts and scattering potential*, Rev. Mod. Phys., 21 (1949), pp. 488–493.

[9] A. Hasenfeld, *SHARP biomedical NMR spatial localization*, Magn. Reson. Med., 2 (1985), pp. 505–511.

[10] A. Abragam, *The Principles of Nuclear Magnetism*, Oxford University Press, London, 1961.

[11] L.D. Landau and E.M. Lifshitz, *Quantum Mechanics (Non-relativistic theory), Third edition*, Pergamon Press, New York, 1977, p. 60.

[12] S. Flügge, *Practical Quantum Mechanics*, Springer-Verlag, Berlin, 1971, p. 94.

FIGURE CAPTIONS.

Figure 1: The N=2 reflectionless potential determined from the data $(\lambda_1, \lambda_2, \phi_1, \phi_2)$=(2.0,1.9,-4.1,2.7) with -μ=10,40 at the top is used in the ansatz (3.15) as an inverting pulse, where the response -M_z is displayed as a function of resonance offset $\frac{\Delta\omega}{\omega_1^o}$ at bottom.

Figure 2: The N=3 reflectionless potential determined from the data $(\lambda_1, \lambda_2, \lambda_3, \phi_1, \phi_2, \phi_3, \phi_4)$= (3.3,2.0,0.8,0.2,-0.3,0.25,-0.39) with -μ=5,10 at the top is used in the ansatz (3.15) as an inverting pulse, where the response -M_z is displayed as a function of resonance offset $\frac{\Delta\omega}{\omega_1^o}$ at bottom.

Figure 3: Everything is the same as in Figure 1, except that the small eigenvalue moves from $\lambda_2 = 1.9 \rightarrow$1.99, and -$\mu$=6.

Figure 4: The eigenvalue data is the same as in Figure 2, but now the phases have moved $(\phi_1, \phi_2, \phi_3, \phi_4) = (0.2, -0.3, 0.25, -0.39) \rightarrow$ (2.3,-1.6,3.1,-4.09) to better separate the solitons, with -μ=10.

Figure 5: The N=2 reflectionless potential determined from the data $(\lambda_1, \lambda_2, \phi_1, \phi_2)$=(2.0,1.9,2.7,2.7) with -μ=8 at the top is used in the ansatz (3.15) as an inverting pulse for $\mid \omega_1 \mid$=25.14,101.1, where the response -M_z is displayed as a function of resonance offset $\frac{\Delta\omega}{\omega_1^o}$ at bottom.

(More details on notation are available for the N=2 and N=3 cases in [4] and [3], respectively, and $\frac{\Delta\omega}{\omega_1^o}$ denotes the average pulse height).

Figure 1

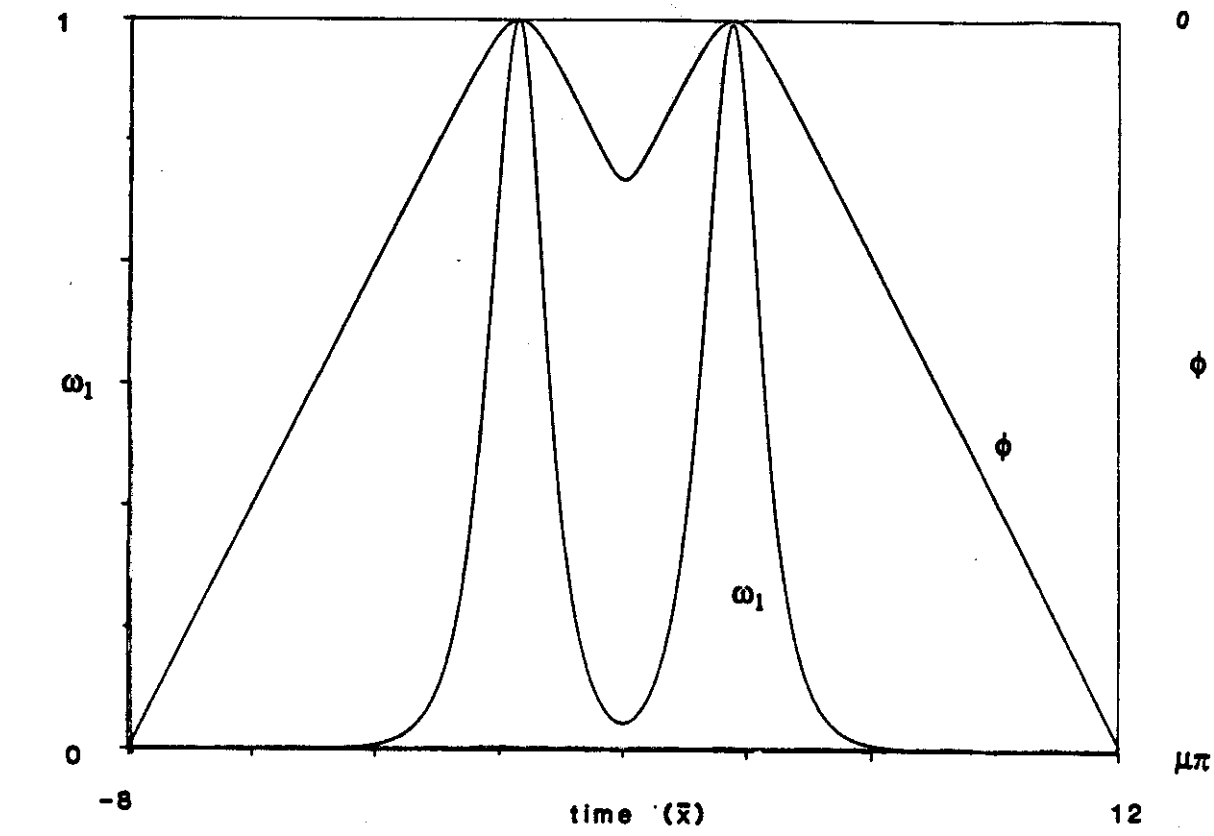
1
0
ω_1
0
ϕ
$\mu\pi$
ϕ
ω_1
-8
time ($\bar{x}$)
12

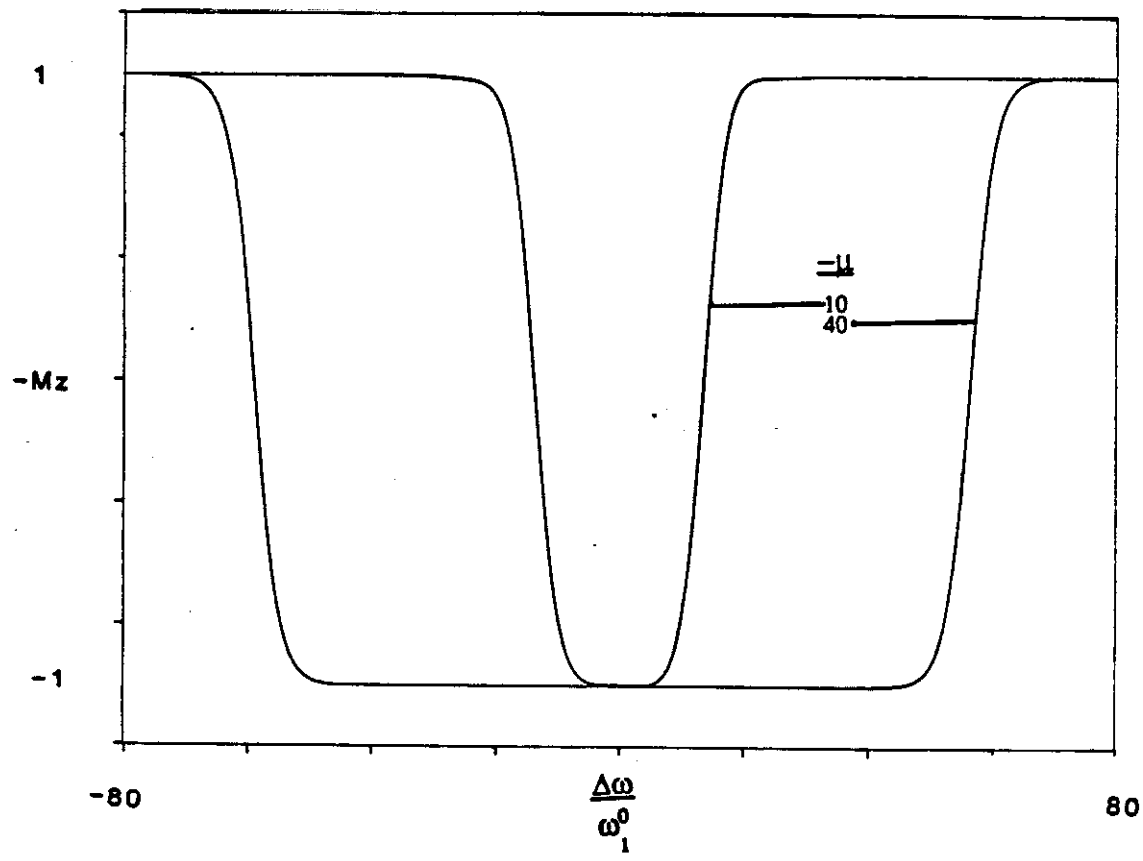
1
-Mz
-1
=μ
10
40
-80
$\frac{\Delta\omega}{\omega_1^0}$
80

Figure 2

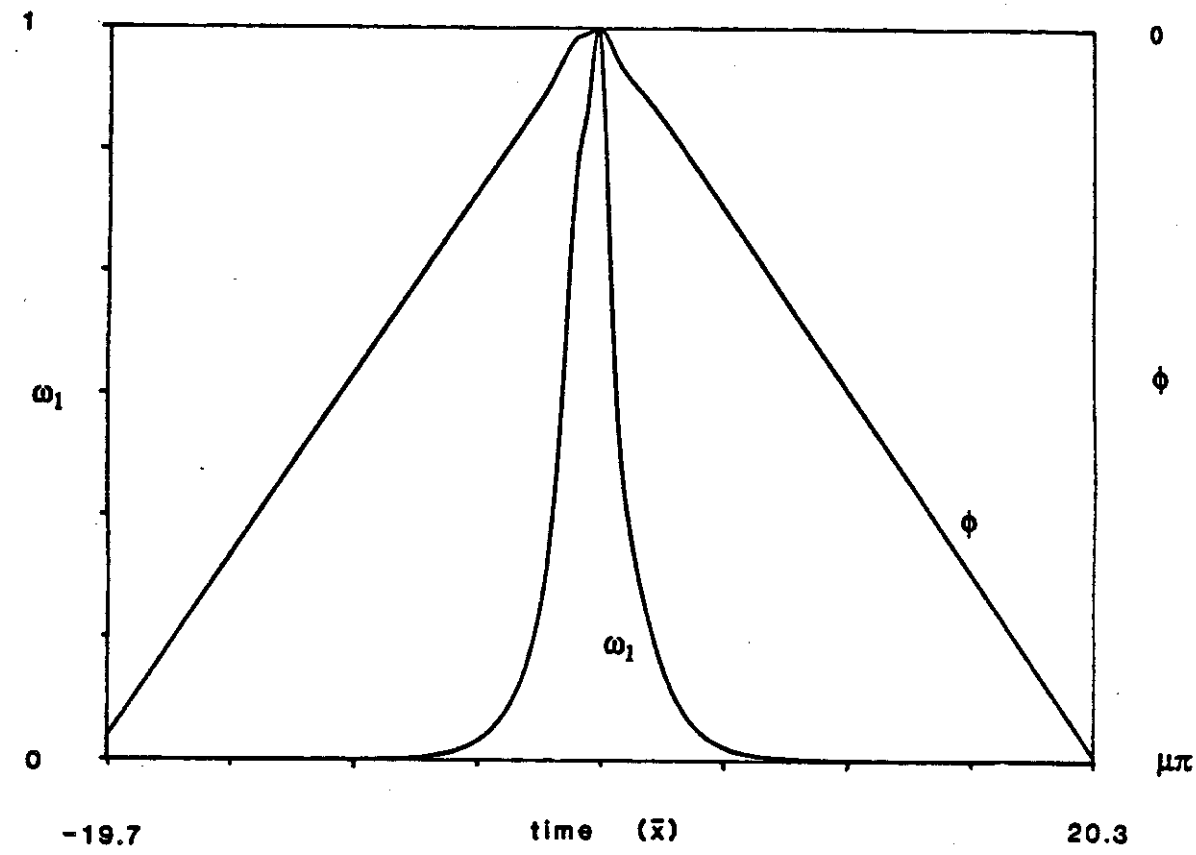
1
0
ω_1
ϕ
0
$\mu\pi$
ϕ
ω_1
-19.7
time ($\bar{x}$)
20.3

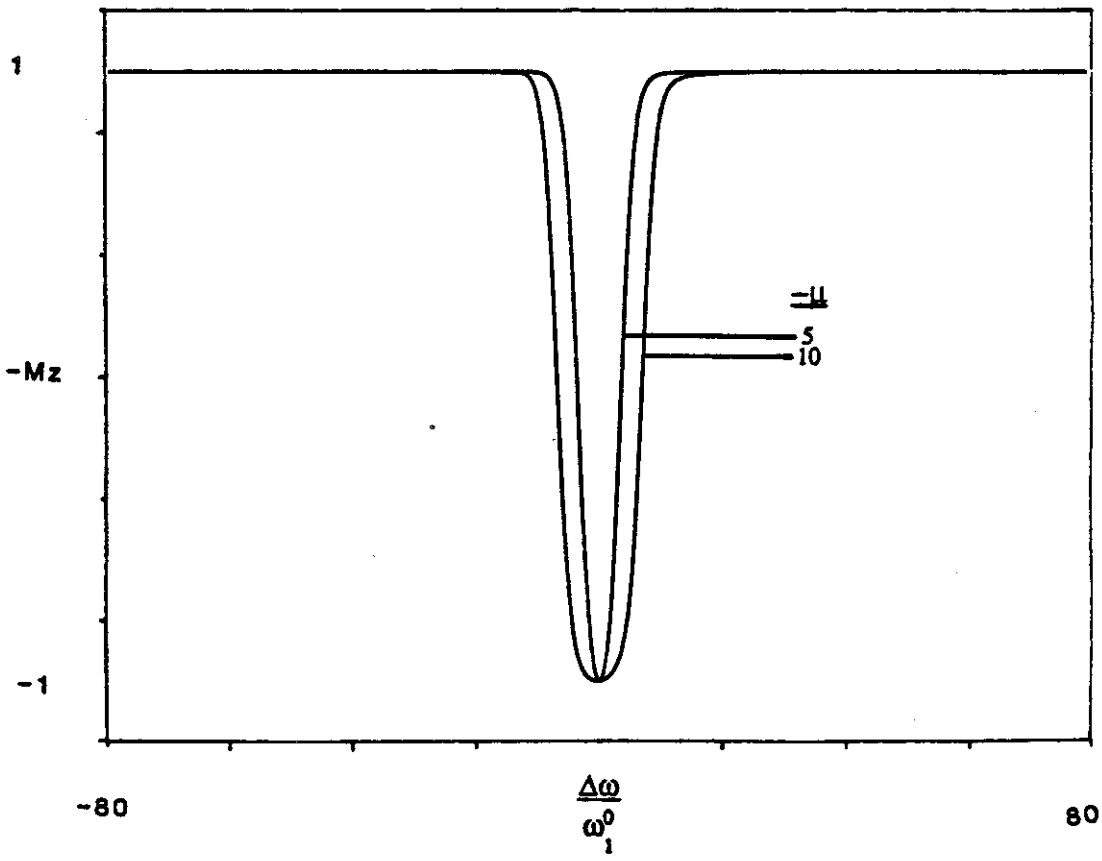
1
-Mz
-1
$=\mu$
5
10
-80
$\frac{\Delta\omega}{\omega_1^0}$
80

Figure 3

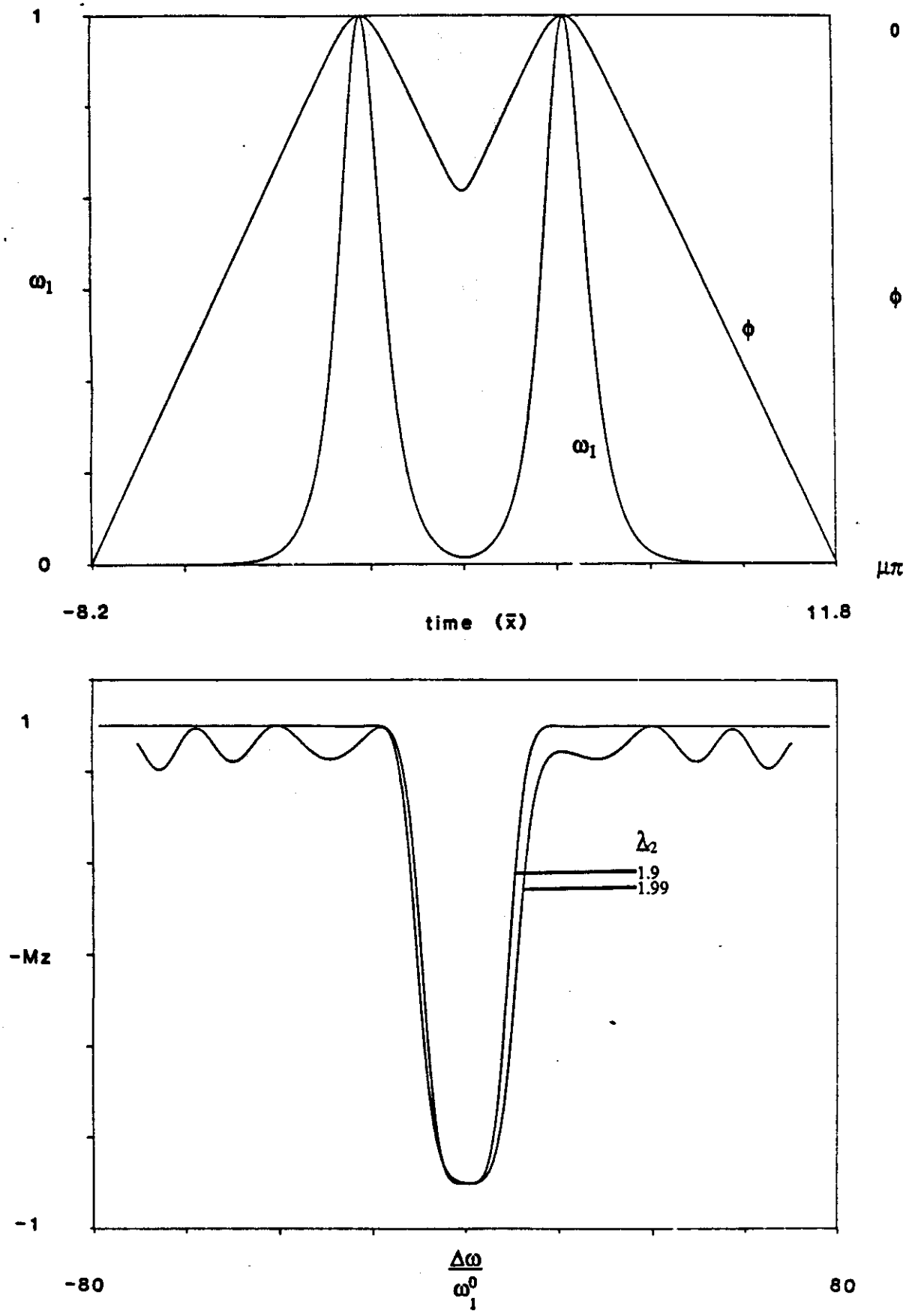
1
0
ω_1
ϕ
ω_1
ϕ
0
$\mu\pi$
-8.2
time ($\bar{x}$)
11.8
1
-Mz
-1
λ_2
1.9
1.99
$\frac{\Delta\omega}{\omega_1^0}$
-80
80

Figure 4

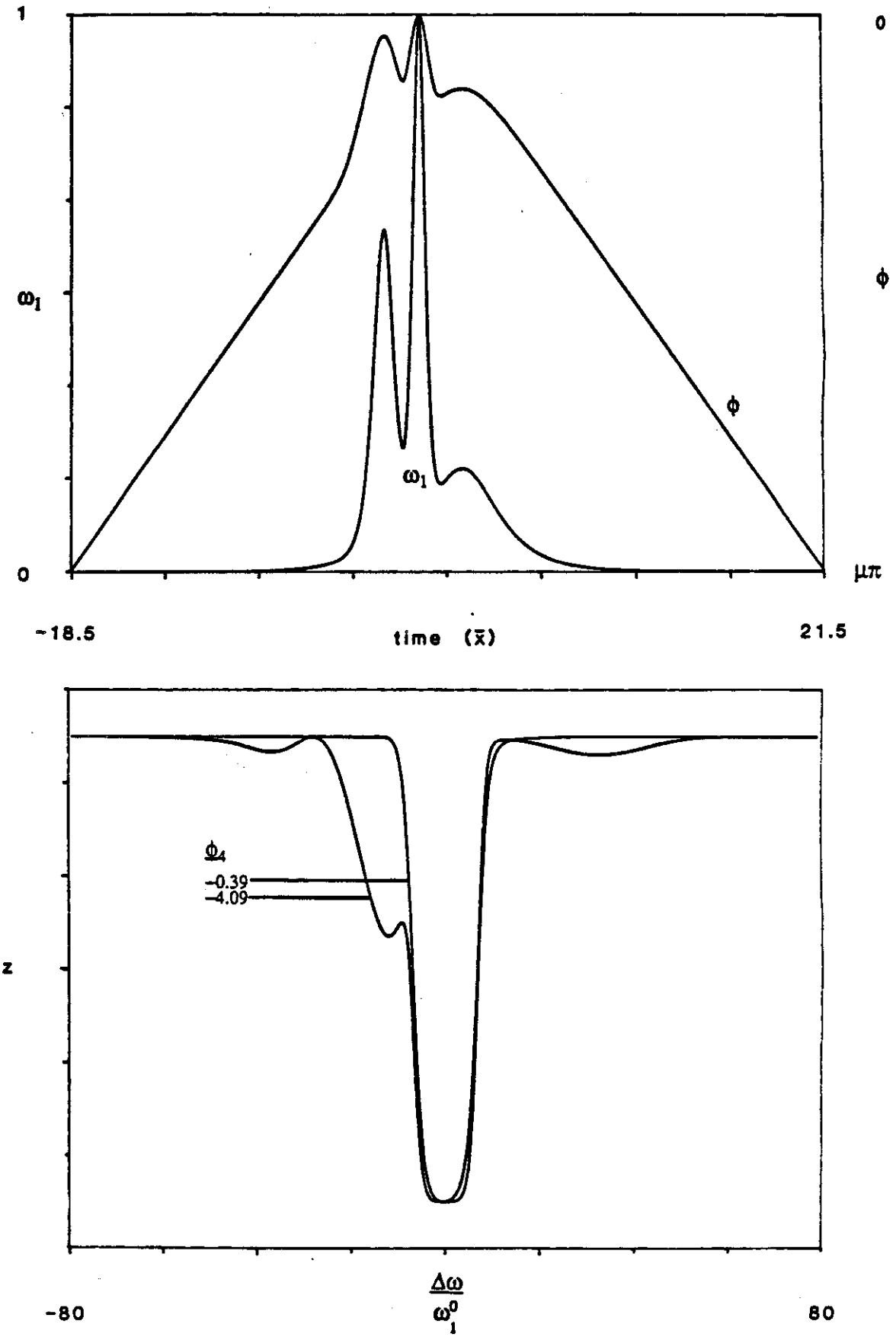
1
0
ω_1
ϕ
ω_1
0
$\mu\pi$
-18.5
time ($\bar{x}$)
21.5
1
Φ_4
-0.39
-4.09
-Mz
-1
$\frac{\Delta\omega}{\omega_1^0}$
-80
80

Figure 5

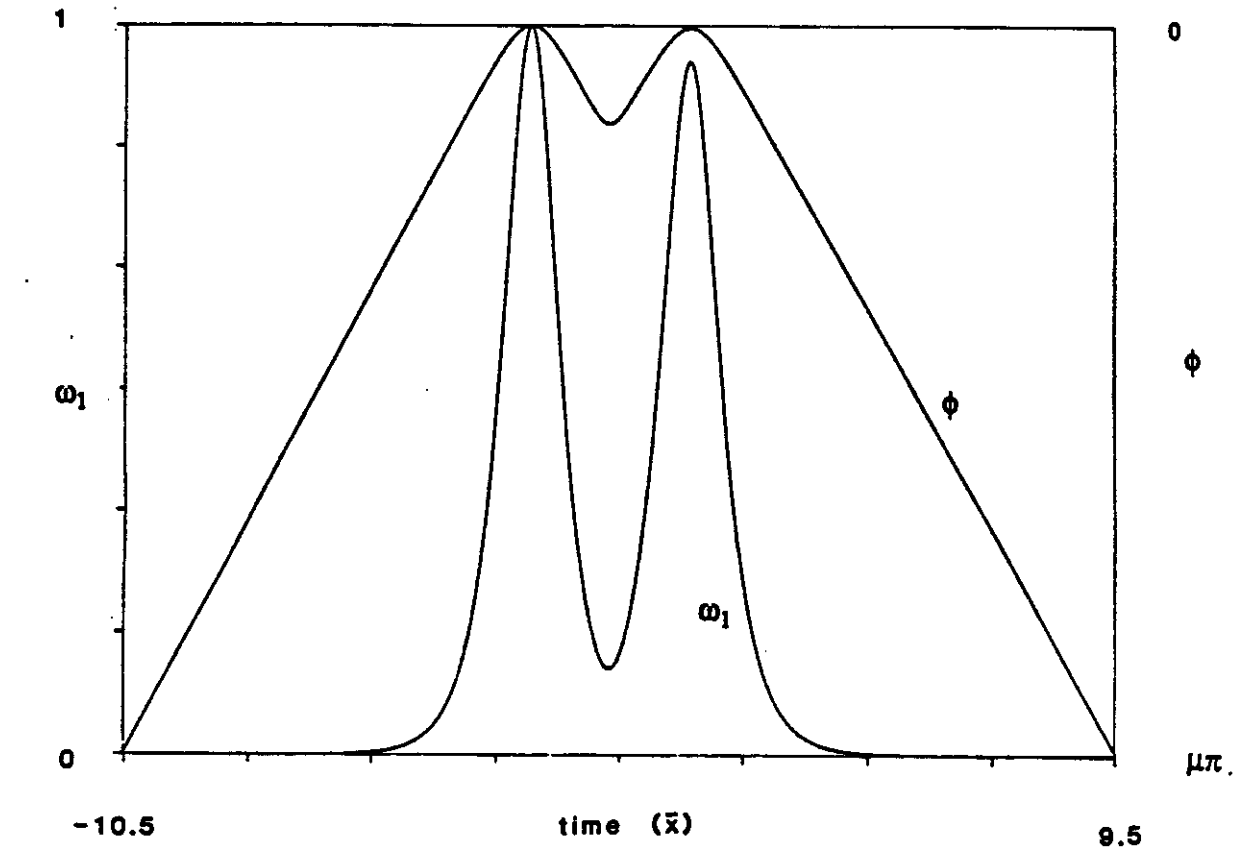
1
0
ω_1
ϕ
ω_1
0
$\mu\pi$
-10.5
time ($\bar{x}$)
9.5

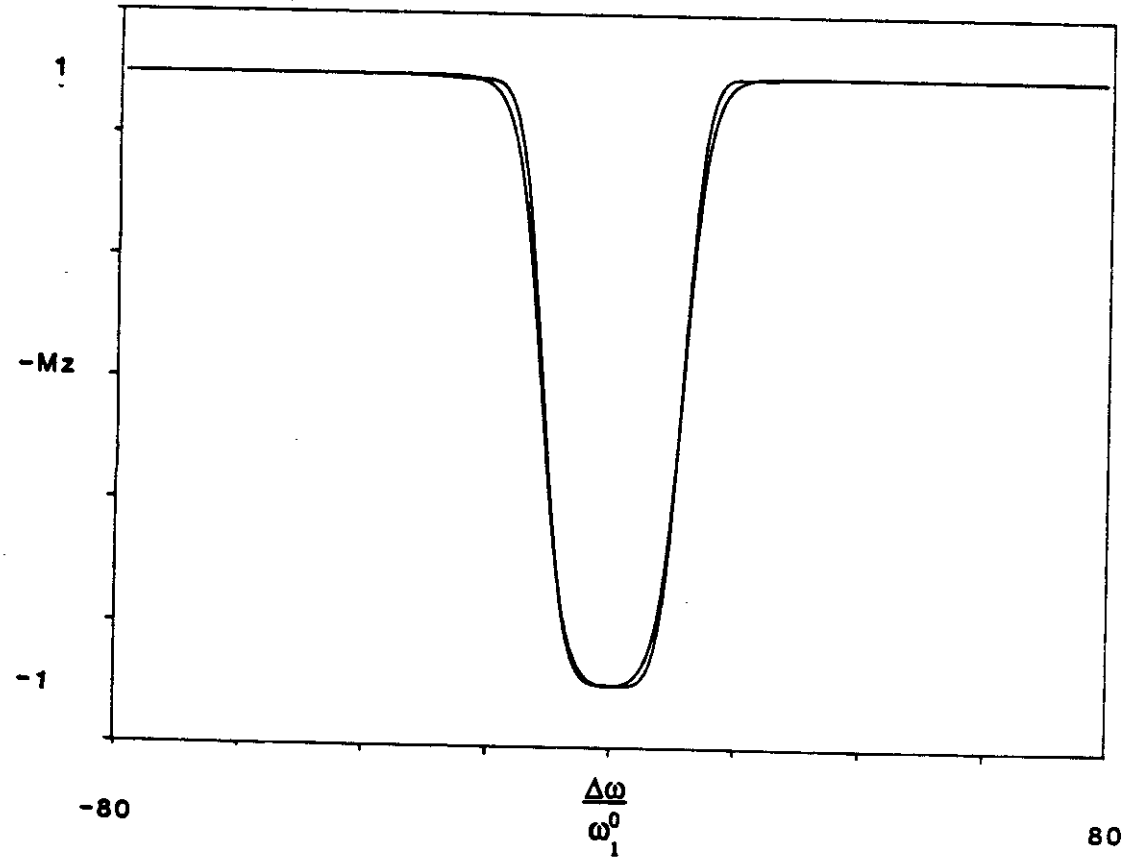
1
-Mz
-1
-80
$\frac{\Delta\omega}{\omega_1^0}$
80